*The paper was presented at the Tenth Meeting*
*"New Trends in Fatigue and Fracture" (NT2F10)*
*Metz, France, 30 August–1 September, 2010*

*Diego Alvarez[1], Alexandre Barbas[2], Anne-Sophie Bonnet[1], Paul Lipinski[1]*

# MEASUREMENT AND INTERPRETATION OF VISCOUS INTERACTIONS DURING CONTACT BETWEEN BONE AND PROSTHETIC MATERIALS

# MERENJE I INTERPRETACIJA VISKOZNIH INTERAKCIJA PRI MEĐUSOBNOM KONTAKTU KOSTI I PROTETIČKIH MATERIJALA

Originalni naučni rad / Original scientific paper
UDK /UDC: 577.353
Rad primljen / Paper received: 31.01.2011

Adresa autora / Author's address:
[1)] Laboratoire de Mécanique, Biomécanique, Polymère, Structures (LaBPS), Ecole Nationale d'Ingénieurs de Metz – Université Paul Verlaine de Metz, Metz, France
[2)] Orthopédie Biomécanique Locomotion, Chatillon, France, a.barbas@enim.fr

**Keywords**
- interactions modelling
- friction coefficient
- friction viscosity
- bone wear

**Ključne reči**
- modeliranje interakcija
- koeficijent trenja
- viskoznost
- trošenje kostiju

*Abstract*

*The design of reliable prosthetic solutions requires wide knowledge of the contact interactions existing inside human joints. Biotribology is of major interest to understand the various mechanisms encountered during this type of contact. The aim of the present work is to propose a new method of experiments and interpretation of the contact existing between bone and a prosthetic material. Firstly, a new tribometer is developed to reproduce this type of contact in vitro, under conditions similar to physiological ones. The experimental tests enabled to quantify bone wear and to determine global interaction forces. Secondly, a rheological model is proposed to identify the frictional and viscous parts of this global interaction force. An example of measurement is detailed in this paper in order to illustrate the fitting of the simulated results to the experimental ones. The values of the rheological parameters corresponding to the best fitting are provided. Thanks to this approach, several conclusions are drawn, allowing to deepen the comprehension of this type of interaction.*

*Izvod*

*Projektovanje pouzdanih protetičkih rešenja zahteva široko poznavanje interakcija pri unutrašnjem kontaktu ljudskih zglobova. Biotribologija je od velikog značaja za razumevanje raznih mehanizama koji se javljaju pri kontaktima ovakvog tipa. Cilj ovog rada je da se predloži nova metoda eksperimenata i interpretacija kontakta koji se javlja između kosti i protetičkog materijala. Pre svega, razvijen je novi tribometar za reprodukovanje kontakata ovakvog tipa in vitro, u uslovima sličnim fiziološkim. Eksperimentalna ispitivanja su omogućila kvantifikovanje trošenja kostiju i određivanje globalnih sila interakcije. Osim toga, predložen je reološki model radi identifikacije frikcionih i viskoznih elemenata ove globalne sile interakcije. Primer izvedenog merenja je detaljno predstavljen u ovom radu radi predstavljanja poklapanja simuliranih i eksperimentalnih rezultata. Date su vrednosti reoloških parametara koji se najbolje poklapaju. Zahvaljujući ovom pristupu, izvedeno je nekoliko zaključaka, koji produbljuju razumevanje interakcija ovakvog tipa.*

## INTRODUCTION

Failure of prosthetic solutions is frequently attributed to the premature wear of contacting materials. Prosthetic concepts are today designed in order to minimize the trauma undergone by the patients during surgery. The last tendency, for instance in the case of joints pathologies, is to carry out a partial replacement of the joint by only substituting the damaged anatomic area by a prosthetic part, /1, 2/. So, the problem of direct contact between a prosthetic material and bone arises. Among the available biocompatible materials, the most often used for this type of application are titanium alloys, stainless steels, ceramics and polymers. However the abrasion of prosthetic materials represents a threat for the patients' health and bone wear generally leads to serious complications. The main goal of this paper is therefore to propose an experimental analysis to measure the interaction forces and the wear rate of bone, submitted to a frictional contact with some of these materials. The contact conditions have to be as representative as possible of the *in vivo* situation in terms of physiological liquid, specific temperature, contact velocity or pressure. The development of an adequate experimental technique is crucial for these purposes. Many tribometers have been designed to study friction coefficients under static or dynamic conditions. An exhaustive overview of these solutions has been made by Philippon et al., /3/. However, they do not meet the requirements mentioned above. For this reason a specific device has been developed for this study.

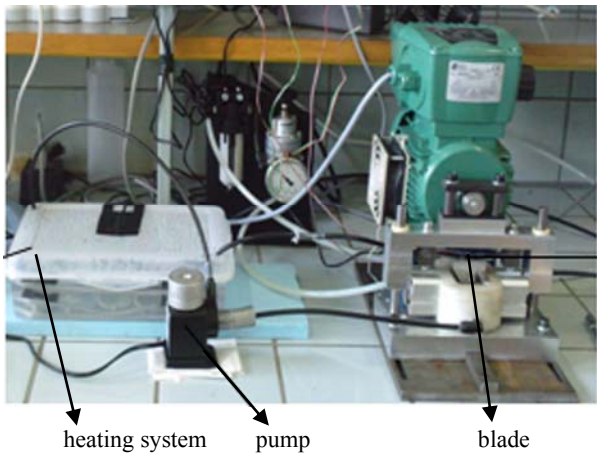


Figure 1. Apparatus used.
Slika 1. Primenjeni uređaj

Figure 1 illustrates the apparatus used in this study. It is composed of the tribometer performing a cyclic loading with controlled sliding amplitude and velocity under the desired contact pressure. The heating system and mini-pump guarantee the physiological liquid rate of flow and bath temperature of immerged interacting specimens. A blade equipped with two gauges enables the determination of friction forces from strain records, /4/. In order to establish the friction coefficient and damping, as well as the friction path length, an accurate interpretation of these records has to be carried out. To this end, a rheological model of the tribometer has been developed. The differential equations obtained have been treated numerically by means of the finite difference method. The experimental records are compared with series of simulated curves. The best fitting one has been used to specify the contact interaction parameters.

## VISCOELASTIC MODEL OF TRIBOMETER

The tribometer is composed of a rigid frame, a cylindrical cam rotating at a given rotation velocity $\omega$ around point $O$. The distance between the cam centre $O'$ and rotation centre $O$ is noted $e$ and called eccentricity, see Figure 2.

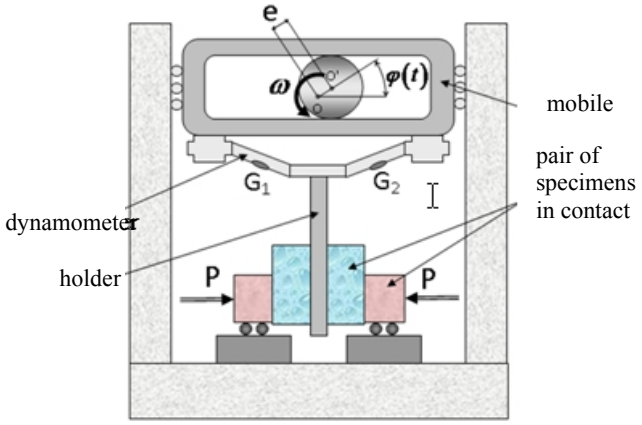


Figure 2. Schematic representation of the tribometer.
Slika 2. Šematski prikaz tribometra

The rotating cam induces the alternative rectilinear motion of a mobile guided by the frame. The blade equipped with the two gauges $G_1$ and $G_2$ enables the measurement of the force inducing the motion of the rigid holder of a pair of prosthetic material samples. Two bone specimens are in contact with these samples under the given normal contact force $P$.

*Interactions*

The interaction between bone specimens and prosthetic material corresponds to the so-called persistent contact due to the external normal contact force $P$ which maintains the bodies in touch. Persistent contact is usually modelled by a spring–damper association where the spring stiffness and the damping describe the elasticity of contacting bodies and the viscous dissipation of energy respectively. The friction law of Coulomb is used to define the contact friction force $Y$. The usual Coulomb law can be written as follows:

$$Y = \mu P \tag{1a}$$

or dividing this last equation by contact surface area $A$:

$$\tau = \mu\sigma \tag{1b}$$

where $\sigma$ and $\tau$ are normal and shear stress components.

We suppose that the current friction coefficient $\mu$ evolves with slip velocity $V_S$, i.e. relative velocity of two contacting bodies. Static $\mu_s$ and dynamic $\mu_d$ friction coefficients are introduced to describe this evolution. The following function is introduced:

$$\mu(V_S) = \mu_s - (\mu_s - \mu_d)\frac{V_S}{V_T + V_S} \tag{2}$$

where $V_T$ is the friction transition velocity. Thus, three contact parameters are introduced to define the contact friction force $Y$, namely $\mu_s$, and $\mu_d$ and $V_T$. One of the aims of this work is to determine these parameters.

*Rheological model*

The interactions between the pair of contacting materials is defined by a rheological model composed of a slider with the friction coefficient $\mu$ in parallel with a dashpot of viscosity $\eta_I$. A spring of stiffness $k_I$ is added to describe the interaction elasticity. The moving mass attached to the dynamometer is noted $M$. This one corresponds to the sum of masses of the holder, the two mobile specimens and the blade. The blade stiffness is designated by $k_D$. Since the junctions between the dynamometer and the mobile are usually not perfect, another dashpot with viscosity $\eta_D$ is introduced to take into account the corresponding energy dissipation. The resulting rheological model of tribometer is illustrated in Fig. 3a.

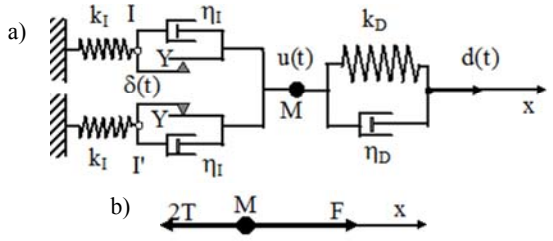


Figure 3. (a) Rheological model, (b) Representation of actions applied to mass $M$.
Slika 3. (a) Reološki model, (b) Shema sila koje deluju na masu $M$

It is obvious, according to Fig. 3a, that the force $F$ measured by the dynamometer corresponds to the sum of the frictional, viscous and inertia forces of the masses in motion. To separate these components and determine the friction coefficients and wear path length, a differential equation of motion is established and resolved numerically using the implicit finite difference method.

## MEASUREMENT SIMULATION

### *Equation of motion*

As illustrated in Fig. 3b, the mass $M$ is submitted to the action of the force $F$ measured by the dynamometer and to the one of the two interaction forces $T$. The corresponding equation of motion takes the following form:

$$M\frac{d^2u}{dt^2}=F-2T \tag{3}$$

where $u(t)$ is the moving mass displacement. Let $d(t)$ be the mobile displacement defined by the rotation velocity $\omega$, the eccentricity $e$ and cam initial angular position $\varphi_0$. This displacement is given by:

$$d(t)=e\sin(\omega t+\varphi_0) \tag{4}$$

Using the usual linear constitutive relations for rheological elements the forces acting on the mass can be expressed as below. The force $F$ is due to the spring and dashpot acting in parallel, so

$$F=F_S+F_A$$

Since $$F_S=k_D\left[d(t)-u(t)\right]$$

and $$F_A=\eta_D\frac{d}{dt}\left(d(t)-u(t)\right)=\eta_D\left(V-\frac{du(t)}{dt}\right)$$

this force becomes:

$$F=k_D\left[d(t)-u(t)\right]+\eta_D\left(V-\frac{du(t)}{dt}\right) \tag{5}$$

where $$V=e\omega\cos(\omega t+\varphi_0) \tag{6}$$

is the known mobile velocity.

On the other hand, the interaction force $T$ is defined by the spring of stiffness $k_I$ describing the elastic part of contact interactions.

$$T=k_I\delta(t) \tag{7}$$

In this expression, $\delta(t)$ is the spring elongation, see Fig. 3b. Let $V_S$ be given by:

$$V_S(t)=\frac{d}{dt}\left(u(t)-\delta(t)\right) \tag{8}$$

Two particular cases have to be considered. The first one corresponds to the situation of slider and associated dashpot at rest ($V_S(t) = 0$), i.e. when:

$$T\le \mathrm{Y} \tag{9}$$

In this case the following expression is obtained:

$$\frac{du(t)}{dt}=\frac{d\delta(t)}{dt} \tag{10}$$

For the active slider ($V_S(t) \neq 0$), i.e. when:

$$|T|>Y \tag{11}$$

the slip velocity is controlled by the dashpot in such manner that:

$$V_S(t)\eta_I=\begin{cases}T-Y & \text{quand} \quad T>0\\ T+Y & \text{quand} \quad T<0\end{cases}$$

or equivalently using Eq.(8)

$$\eta_I\frac{d}{dt}\left(u(t)-\delta(t)\right)=T-Y\mathrm{sign}(T) \tag{12}$$

Equations (10) and (12) define the relationship between $\delta(t)$ and $u(t)$ for both cases, respectively.

The nonlinear equation of motion takes the final form:

$$M\frac{d^2u}{dt^2}=k_D\left[d(t)-u(t)\right]+\eta_D\frac{d}{dt}\left[d(t)-u(t)\right]-2k_I\delta(t) \tag{13}$$

This equation, combined with (10) or (12), is solved numerically using the implicit version of finite difference method.

### *Finite difference formulation*

In the finite difference method, the following approximations of differential operators are frequently used:

$$\left(\frac{du}{dt}\right)_i\approx\frac{u_{i+1}-u_{i-1}}{2\Delta t} \tag{14}$$

$$\left(\frac{d^2u}{dt^2}\right)_i\approx\frac{u_{i+1}-2u_i+u_{i-1}}{\Delta t^2} \tag{15}$$

where $u_i = u(i\Delta t)$, $u_{i-1} = u[(i - 1)\Delta t]$, $u_{i+1} = u[(i + 1)\Delta t]$ and $\Delta t$ and $i$ are the time increment and its number respectively. Introducing these approximations into (13) one obtains:

$$\begin{aligned}M\frac{u_{i+1}-2u_i+u_{i-1}}{\Delta t^2}=\\ =k_D(d_{i+1}-u_{i+1})+\eta_D V_{i+1}-\frac{\eta_D}{2\Delta t}(u_{i+1}-u_{i-1})-2k_I\delta_{i+1}\end{aligned} \tag{16}$$

where $V_{i+1}$ is the mobile velocity specified by Eq.(6) and specialized for time $i + 1$. The implicit character of this algorithmic equation is due to the fact that all forces are estimated at time $i + 1$. Two unknown quantities appear in this equation, namely $u_{i+1}$ and $\delta_{i+1}$. To be solved with respect to $u_{i+1}$, this expression has to be accompanied by one of the Eqs.(10) or (12) as a function of the slider activity. This problem can be treated using the predictor-corrector concept. In the predictor step, we suppose the slider to be at rest. In such a situation, the incremental form of Eq.(10) enables the determination of $\delta_{i=1}^{test}$ – a test value of $\delta(t)$ – function of $u_{i+1}$:

$$\delta_{i+1}^{test}=u_{i+1}-u_{i-1}+\delta_{i-1} \tag{17}$$

Introducing (17) into (16) and solving the resulting expression with respect to $u_{i+1}$, the following relationship is obtained:

$$u_{i+1}^{test}=\frac{X_{i+1}^{test}}{K_{eff}^{test}} \tag{18}$$

where $$K_{eff}^{test}=k_D+2k_I+\frac{M}{\Delta t^2}+\frac{\eta_D}{2\Delta t} \tag{19}$$

$$X_{i+1}^{el}=k_D d_{i+1}+\eta_D V_{i+1}+\frac{M}{\Delta t^2}(2u_i-u_{i-1})+\frac{\eta_D}{2\Delta t}u_{i-1}+2k_I(u_{i-1}-\delta_{i-1}) \tag{20}$$

It can then be tested if this test solution respects the condition (9) of slider at rest. For this reason, the test value of interaction force is computed:

$$T_{i+1}^{test} = k_I \delta_{i+1}^{test}$$

If this value verifies the following inequality:

$$\left| T_{i+1}^{test} \right| \le Y_{i+1}$$

then the test solution becomes a new solution of the problem:

$$u_{i+1} = u_{i+1}^{test} \tag{21}$$

if not, the correction step has to be performed and Eq.(12) is used to determine a corrected value of $\delta_{i+1}$.

$$\delta_{i+1} = \frac{1}{2\Delta t k_I + \eta_I}\left[\eta_I (u_{i+1} - u_{i-1} + \delta_{i-1}) + 2\Delta t Y_{i+1} \mathrm{sign}(T_{i+1}^{el})\right] \tag{22}$$

Combining this relationship with (16) and solving the resulting expression with respect to $u_{i+1}$ yields:

$$u_{i+1} = \frac{X_{i+1}}{K_{eff}} \tag{23}$$

where

$$K_{eff} = K_{eff}^{test} - 4k_I \Delta t \frac{k_I}{2\Delta t k_I + \eta_I} \tag{24}$$

$$X_{i+1} = X_{i+1}^{test} - \frac{4k_I \Delta t}{2\Delta t k_I + \eta_I}\left[k_I (u_{i-1} - \delta_{i-1}) + Y_{i+1} \mathrm{sign}(T_{i+1}^{el})\right] \tag{25}$$

are the corrected values of their test Eqs.(19) and (20). A Fortran programme is written to simulate the measurements obtained with the device presented above.

## APPLICATION TO BONE WEAR MEASUREMENTS

### *Experimental results*

A typical wear test of bone in contact with Yttrium Stabilized Zirconium plates is analysed here. The bone specimens are cut off from the cortical diaphysal part of a young pig femur. These parallelepiped specimens of 10 × 12 mm$^2$ cross section are preserved following the appropriate conservation protocol. A groove of 2 mm width and 1 mm depth is machined on the specimen in a direction parallel to the motion axis. This groove enables wear measurements. The experimental conditions of wear test are resumed in Table 1. Specimens have been oriented in such a manner that the direction of femur axis is parallel to the holder movement.

Table 1. Test parameters.
Tabela 1. Parametri ispitivanja

| Specimen orientation | P (N) | $\omega$ (Hz) | $e$ (mm) | $T$ (°C) | Fluid nature |
|---|---|---|---|---|---|
| \| \| | 300 | 3.50 | 4 | 37 | bovine serum |

Figure 4 shows a typical experimental record of strain versus time obtained during one second of this wear test. Approximately three cycles have been recorded showing a similar and repetitive behaviour of both gauges, even if the strain magnitudes are different. Knowing the calibration factors of these gauges the evolution of force $F$ can be drawn. This force is represented in Fig. 5 for one cycle of wear. This graph is used in the next section to identify the contact interaction parameters.

### *Interpretation of contact interactions*

The model developed in the previous section requires data describing the tribometer and the contact interactions as well as the test conditions. The necessary data concerning the test conditions are recapitulated in Table 1. To characterise the tribometer, the measures of blade stiffness $k_D$ and moving mass $M$ are performed. The blade stiffness is estimated to be $k_D = 1.316 \cdot 10^6$ Nm$^{-1}$ and the mass $M =$ 0.107 kg. Since the dynamometer is strongly screwed to the mobile, it is supposed as a first order approximation that the dynamometer damping is nil, $\eta_D = 0$ Nsm$^{-1}$. The remaining parameters, i.e. the static and dynamic friction coefficients, the friction transition velocity and the contact stiffness and damping, have to be determined by fitting of the experimental curve in Fig. 5.

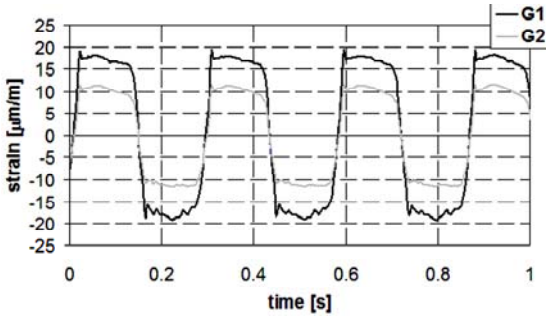


Figure 4. Records of the 2 strain gauges on the blade during 1 s.
Slika 4. Deformacije sa 2 merne trake na lopatici u toku 1 s

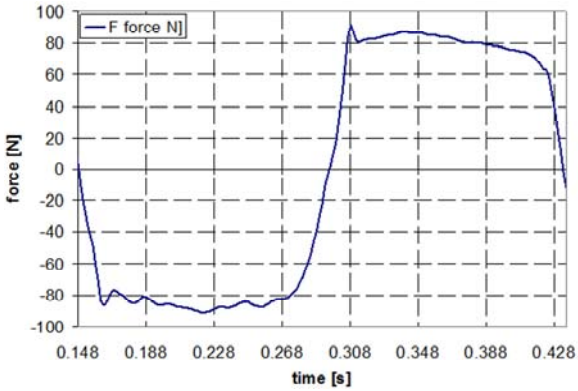


Figure 5. Evolution of the force $F$ measured by the dynamometer as a function of time for one cycle.
Slika 5. Razvoj sile $F$ izmerena dinamometrom kao funkcija vremena za jedan ciklus

First, the static friction coefficient $\mu_s$ is determined. To this end, static and dynamic coefficients are supposed to be identical. In such a situation the friction transition velocity becomes inactive. Besides, the interaction damping is supposed to be nil, ($\eta_I = 0$ Nsm$^{-1}$), and the interaction stiffness very large ($k_I = 1.316 \cdot 10^{20}$ Nm$^{-1}$). The value of static friction coefficient is chosen to obtain a force $F$ applied by the dynamometer of 80 N, corresponding to the beginning of the sliding, see Fig. 5. The value of static friction coefficient fitting well in this event is $\mu_s = 0.135$. The resulting graph of $F$ versus time is shown in Fig. 6a compared with the experimental curve. The next step consists in fitting the contact interaction stiffness. The value of $k_I = 1.5 \cdot 10^5$ Nm$^{-1}$ leads to the graph presented in Fig. 6b. The dynamic friction coefficient and transition velocity are subsequently adjusted. The values leading to the graphs in Fig. 6c are respectively $\mu_D = 0.11$ and $V_T = 2.5 \cdot 10^{-3}$ ms$^{-1}$.

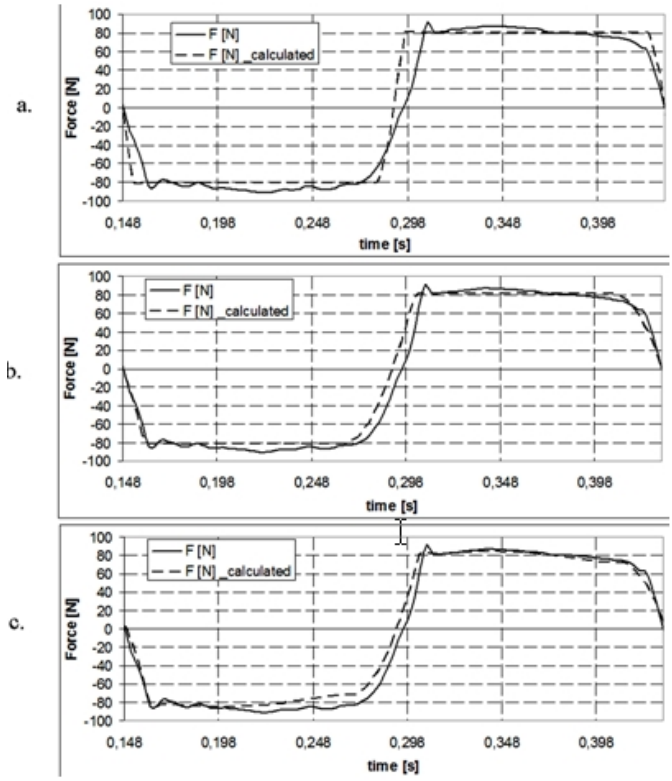


Figure 6. Fitting of the experimental curve: a) static friction coefficient $\mu_s = 0.135$, b) contact interaction stiffness $k_I = 1.5 \cdot 10^5$ Nm$^{-1}$, c) dynamic friction coefficient $\mu_D = 0.11$ and transition velocity $V_T = 2.5 \cdot 10^{-3}$ ms$^{-1}$.

Slika 6. Fitovanje eksperimentalne krive: a) statički koeficijent trenja $\mu_s = 0.135$, b) krutost interakcije kontakta $k_I = 1.5 \cdot 10^5$ Nm$^{-1}$, c) dinamičkog koeficijenta trenja $\mu_D = 0.11$ i prelazne brzine $V_T = 2.5 \cdot 10^{-3}$ ms$^{-1}$

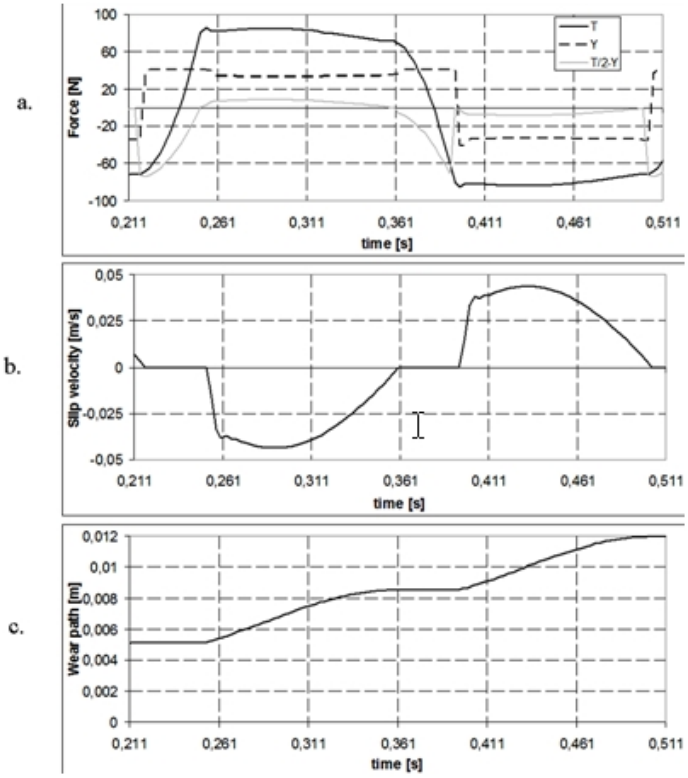


Figure 7. Fitting of the experimental curve: a) static friction coefficient $\mu_s = 0.135$, b) contact interaction stiffness $k_I = 1.5 \cdot 10^5$ Nm$^{-1}$, c) dynamic friction coefficient $\mu_D = 0.11$ and transition velocity $V_T = 2.5 \cdot 10^{-3}$ ms$^{-1}$.

Slika 7. Fitovanje eksperimentalne krive: a) statički koeficijent trenja $\mu_s = 0.135$, b) krutost interakcije kontakta $k_I = 1.5 \cdot 10^5$ Nm$^{-1}$, c) dinamičkog koeficijenta trenja $\mu_D = 0.11$ i prelazne brzine $V_T = 2.5 \cdot 10^{-3}$ ms$^{-1}$

The results of the simulations enable the complete interpretation of the wear test. Figure 7 indicates respectively the interaction force $T$, its frictional $Y$ and viscous $T - Y$ parts (Fig. 7a), the slip velocity $V_S$ (Fig. 7b) and the wear path (Fig. 7c) for a typical cycle. The following remarks can be formulated:

- the loading and unloading parts of force–time (displacement) curve are not symmetric,
- the wear path per cycle is different from twice the eccentricity value,
- the viscous part of interactions for the wet contact of the bone–ceramic pair is as important as the frictional one.

## CONCLUSION

A new tribometer is designed to test the interactions existing during contact between bone and prosthetic materials in conditions close to physiological ones. An original rheological model is proposed to identify the frictional and viscous parts of the interaction force. The frictional coefficient is also determined.

## REFERENCES


1. Lindqvist, C., Söderholm, A.L., Hallikainen, D., Sjövall, L., *Erosion and heterotopic bone formation after alloplastic temporomandibular joint reconstruction*, J Oral Maxillofac Surg, 1992, Vol.50, pp.984-996.
2. Westermark, A., Koppel, D., Leiggener, C., *Condylar replacement alone is not sufficient for prosthetic reconstruction of the temporomandibular joint*, International J of Oral and Maxillofacial Surgery, 2006, Vol.35, pp.488-492.
3. Philippon, S., Voyiadjis, G.Z., Faure, L., Lodygowski, A., Rusinek, A., Chevrier, P., Dossou, E., *A device enhancement for the dry sliding friction coefficient measurement between Steel 1080 and VascoMax with respect to surface roughness changes*, Experimental Mechanics, 2010, pp.1-10.
4. Barbas, A., Bonnet, A.S., Lipinski, P., Philippon, S., *Experimental Study of Wear between Bone and Various Prosthetic Materials*, 23rd European Conference on Biomaterials, Tampere, September 2010.